Journal of Cellular Physiology

The Synergistic Effect of SAHA and Parthenolide in MDA-MB231 Breast Cancer Cells

DANIELA CARLISI,[1] MARIANNA LAURICELLA,[1] ANTONELLA D'ANNEO,[2] GIUSEPPINA BUTTITTA,[1] SONIA EMANUELE,[1] RICCARDO DI FIORE,[2] ROBERTA MARTINEZ,[2] CHRISTIAN ROLFO,[3] RENZA VENTO,[2,4] AND GIOVANNI TESORIERE[1,4]*

[1]*Department of Experimental Biomedicine and Clinical Neurosciences (BioNeC), Laboratory of Biochemistry, Polyclinic, University of Palermo, Palermo, Italy*

[2]*Department of Biological, Chemical and Pharmaceutical Sciences and Technologies (STEBICEF), Laboratory of Biochemistry, Polyclinic, University of Palermo, Palermo, Italy*

[3]*Phase I-Early Clinical Trials Unit, Oncology Department, Antwerp University Hospital, Edegem, Belgium*

[4]*Sbarro Institute for Cancer Research and Molecular Medicine, College of Science and Technology, Temple University, Philadelphia, Pennsylvania*

The sesquiterpene lactone Parthenolide (PN) exerted a cytotoxic effect on MDA-MB231 cells, a triple-negative breast cancer (TNBC) cell line, but its effectiveness was scarce when employed at low doses. This represents an obstacle for a therapeutic utilization of PN. In order to overcome this difficulty we associated to PN the suberoylanilide hydroxamic acid (SAHA), an histone deacetylase inhibitor. Our results show that SAHA synergistically sensitized MDA-MB231 cells to the cytotoxic effect of PN. It is noteworthy that treatment with PN alone stimulated the survival pathway Akt/mTOR and the consequent nuclear translocation of Nrf2, while treatment with SAHA alone induced autophagic activity. However, when the cells were treated with SAHA/PN combination, SAHA suppressed PN effect on Akt/mTOR/Nrf2 pathway, while PN reduced the prosurvival autophagic activity of SAHA. In addition SAHA/PN combination induced GSH depletion, fall in $\Delta\psi m$, release of cytochrome c, activation of caspase 3 and apoptosis. Finally we demonstrated that combined treatment maintained both hyperacetylation of histones H3 and H4 induced by SAHA and down-regulation of DNMT1 expression induced by PN. Inhibition of the DNA-binding activity of NF-kB, which is determined by PN, was also observed after combined treatment. In conclusion, combination of PN to SAHA inhibits the cytoprotective responses induced by the single compounds, but does not alter the mechanisms leading to the cytotoxic effects. Taken together our results suggest that this combination could be a candidate for TNBC therapy.

J. Cell. Physiol. 230: 1276–1289, 2015.

Triple-negative breast cancer (TNBC) refers to a very aggressive subtype of breast carcinomas associated with poor prognosis (Dey et al., 2012). These forms of breast cancers do not express estrogen, progesterone and HER2/neu receptors and are unresponsive to treatment with hormonal therapy or Herceptin (Bauer et al., 2007). Chemotherapy with anthracyclines, taxanes, and platinum agents is the main form of treatment, but is accompanied by a high rate of recidivism (Bayraktar and Glück, 2013). Therefore, a novel treatment strategy founded on the biochemical characteristics of TNBCs is urgently needed.

Parthenolide (PN), the principal bioactive sesquiterpene lactone component of feverfew *Tanacetum parthenium,* exerts anti-tumor activity on several cancer cell types, including prostate (Sun et al., 2010), pancreatic (Liu et al., 2010a) and colorectal cancers (Zhang et al., 2004), multiple myeloma (Suvannasankha et al., 2008), osteosarcoma (D'Anneo et al., 2013a) and melanoma (D'Anneo et al., 2013a), while it shows low toxicity in normal cells. It is noteworthy that PN is the first small molecule found to be active against cancer stem cells (Ghantous et al., 2013). The anti-tumour activity of PN has been primarily correlated with the inhibition of the NF-κB transcription factor (Ghantous et al., 2013). PN has been shown to prevent the DNA binding activity of NF-κB by inhibition of IκB phosphorylation (Kwok et al., 2001). Furthermore, it can inhibit NF-κB activity because causes the alkylation of cysteine sulfhydryl groups in the p65 subunit (García-Piñeres et al., 2004). In addition PN down-regulates the activity of DNA methyltransferase 1 (DNMT1) (Liu et al., 2009), an enzyme involved in DNA methylation, through an inhibition of its expression and a direct covalent binding to the thiol groups in the catalytic site of the enzyme. This results in a significant DNA hypomethylation both in vitro and in vivo.

Conflict of interest: None.

Contract grant sponsor: European Regional Development Fund;
Contract grant number: 2013-PICO-0005.
Contract grant sponsor: Italian Ministry of Education, University and Research (MIUR);
Contract grant number: 2012-ATE-0122.

*Correspondence to: Giovanni Tesoriere, Department of Experimental Biomedicine and Clinical Neurosciences, Laboratory of Biochemistry, Polyclinic, via del Vespro 129, 90127 Palermo, Italy.
E-mail: giovanni.tesoriere@unipa.it

Manuscript Received: 19 September 2014
Manuscript Accepted: 29 October 2014

Accepted manuscript online in Wiley Online Library (wileyonlinelibrary.com): 5 November 2014.
DOI: 10.1002/jcp.24863

Finally, many lines of evidence indicate that PN induces cytotoxic effects in tumour cells by increasing the production of reactive oxygen species (ROS) (D'Anneo et al., 2013a,b; Zunino et al., 2007). Unfortunately, the pharmacologic use of PN is very difficult owing to its scarce solubility. In this regard, recently a dimethylamino-analogue of PN (DMAPT) soluble in ethanol, and its water-soluble derivative, fumarate salt, have been generated, which improve solubility and bioavailability and exhibit an acceptable toxicological profile in animal studies (Guzman et al., 2007). DMAPT eradicates primary leukaemia stem cells and suppresses in vivo the growth of prostate, lung, and bladder cancers (Shanmugam et al., 2010, 2011).

Interestingly, it has been observed that PN and its analogues induce in leukaemia cells a cytoprotective response that reduces the potency of the cytotoxic action exerted by the compounds (Sen et al., 2013). This response represents a limit to the potential use of PN as anti-cancer drug.

We have provided evidence that PN induced a caspase-independent cell death in MDA-MB231 cells (D'Anneo et al., 2013b), a TNBC cell line. This effect was clearly observed at 15–25 μM and was correlated with generation of ROS (D'Anneo et al., 2013b; Carlisi et al., 2014). In addition, we have shown that DMAPT significantly decreased tumour growth in mice bearing xenografts of MDA-MB231 cells, enhanced survival of treated mice and reduced the area of lung metastasis (D'Anneo et al., 2013b). Recently, we have performed new research in order to evaluate compounds capable of sensitizing MDA-MB231 cells to the cytotoxic action of PN. Preliminary results suggest that the suberoylanilide hydroxamic acid (SAHA), an histone deacetylase inhibitor (HDACi), is capable of sensitizing MDA-MB231 cells to the cytotoxic effect of PN.

SAHA has been shown to induce apoptosis in a large spectrum of haematological and solid tumors (Marks and Xu, 2009). In addition, SAHA exerts antitumor effects in a synergistic manner with various compounds such as topoisomerase inhibitors (Guerrant et al., 2012), proteasome inhibitors (Emanuele et al., 2007) and TRAIL (Lauricella et al., 2012). Furthermore, clinical investigations have provided evidence that SAHA exhibited a high therapeutic potential for different forms of tumors at doses that were well tolerated by patients (Slingerland et al., 2014). Moreover, SAHA has been approved by the "Food and Drug Administration" for therapy in patients with haematological malignancies. Previously, we have demonstrated that SAHA induced apoptosis in MDA-MB231 cells (Lauricella et al., 2012). The results of the present paper indicate that pre-treatment of MDA-MB231 cells with SAHA sensitizes the cells to the cytotoxic effect of PN.

Materials and Methods

Chemicals and reagents

PN was supplied by Sigma-Aldrich (Milan, Italy), while SAHA was generously provided by Italfarmaco (Milan, Italy). Stock solutions of both compounds were prepared in dimethyl sulfoxide (DMSO) and diluted to final concentration in the culture medium. DMSO employed as vehicle never exceeded 0.04% of total incubation volume and did not show any toxic effects on MDA-MB231 cells in comparison with the control. All reagents except for z-VAD-fmk, which was supplied from Promega (Milan, Italy), were purchased from Sigma-Aldrich.

Cell cultures

Breast carcinoma MDA-MB231 cells supplied from "Istituto Scientifico Tumori" (Genoa, Italy) were grown as monolayer in Dulbecco's Modified Eagle Medium (DMEM) supplemented with 10% fetal calf serum (FCS), 2 mM glutamine and 1% non essential amino acids, at 37°C in a humidified atmosphere containing 5% CO_2. Before each experiment, cells were seeded in 96 or 6-well plates and were allowed to adhere overnight, then were treated with chemicals or vehicle only.

Detection of cell death

Cell viability was ascertained by MTT method, a colorimetric assay for measuring the activity of mitochondrial dehydrogenases that reduce the tetrazolium dye, MTT, to formazan. The absorbance of the formazan was measured directly at 490 nm in a 96-well plate, using an automatic ELISA plate reader (OPSYS MR, Dynex Technologies, Chantilly, VA) as previously described (D'Anneo et al., 2013b). Apoptotic and necrotic effects were identified by staining with fluorescein isothiocyanate-conjugated (FITC)-Annexin V and propidium iodide (PI) using a commercial kit (BD Biosciences Pharmingen, San Diego, CA) and following the manufacturer's directions. Fluorescence of the cells (10^5 per condition) was analysed by flow cytometry on a Beckman Coulter Epics XL flow cytometer (Brea, CA) and data were analysed by Expo32 software.

Analysis of reactive oxygen species (ROS)

The generation of intracellular reactive oxygen species (ROS) was detected using the cell-permeant 5-(and-6)-carboxy-2′,7′-dichlorodihydrofluorescein diacetate (H_2-DCFDA, Molecular Probe, Life Technologies, Eugene, OR), a fluorogenic dye that easily diffuses across cell membranes becoming oxidized by ROS. Following the incubation of cells (8×10^3/well) with drugs for various times, the medium was replaced with 100 μl of 50 μM H_2-DCFDA in HBSS (Hank's Salt Balanced Solution) and incubation was protracted for 30 min at 37°C in the dark. Then the dye was removed and 100 μl PBS were added. After 20 min the fluorescence was directly detected by means of a fluorescence microscope using a FITC filter with an excitation and an emission wavelength of 485 nm and 530 nm, respectively. To determine the percentage of cells producing reactive oxygen intermediates, cells with green fluorescence were counted and the values were normalized to the total cell count/field. At least 5 fields/condition were analyzed.

Measurement of GSH content

The intracellular GSH level was measured using a commercial assay provided by OXIS Research (Portland, OR). Briefly, after treatment with compounds, the cells (5×10^5/condition) were collected and centrifuged at 120 *g* for 8 min. The pellets were resuspended in 50 μl metaphosphoric acid (5 g/100 ml distilled water) and centrifuged at 3000 *g* for 10 min. GSH content was measured as described by manufacturer's instructions. Absorbance was read at 400 nm in a 96-well plate reader (OPSYS MR, Dynex Technologies, Chantilly, VA). Intracellular GSH content was reported as nanomoles of GSH per 10^5 cells.

Measurement of NF-kB activity

NF-kB activity was evaluated by an Elisa-based assay (Trans-AM NF-kB; Active Motif, Carlsbad, CA) as described by manifacture's protocol. Nuclear extracts were prepared as previously reported (D'Anneo et al., 2013a), using 3×10^5 cells/condition. Aliquots were placed in 96-well plates coated with an oligonucleotide containing the NF-kB consensus sequence. NF-kB activity was detected using a specific antibody for p65 subunit provided by the kit (D'Anneo et al., 2013b).

Labeling of autophagic vacuoles by monodansylcadaverine

Following treatment with compounds, the cells (8×10^3/well) were incubated with 0.05 mM monodansylcadaverine (MDC) in

PBS at 37°C for 10 min in the darkness (Biederbick et al., 1995). Then, cells were washed twice with PBS and immediately analysed by fluorescence microscopy using a Leica DMR inverted microscope equipped with a DAPI filter system (excitation wavelength of 372 nm and emission wavelength of 456 nm). Images were obtained with a CCD camera and processed using the Leica Q Fluoro Software (Wetzlar, Germany).

Western blotting analysis

Whole cell lysates were prepared as previously reported (Carlisi et al., 2011) and protein concentration was determined by Lowry assay (Lowry et al., 1951). As far as cytochrome c analysis, mitochondrial and cytosolic fractions were prepared as previously reported (D'Anneo et al., 2013a). Equal amounts of protein samples (50 μg/lane) were run in a SDS polyacrylamide gel electrophoresis, then transferred to a nitrocellulose membrane. All analyses were performed using specific primary antibodies which were provided by Santa Cruz Biotechnology (Santa Cruz, CA), except for LC-3 which was from Novus Biologicals (Littleton, CO), phospho-mTOR, beclin-1, phospho-p70S6K, p21, p27, cytochrome c, and caspase 3 which were from Cell Signaling Technology (Beverly, MA) and ULK1/2, DNMT1 and β-actin from Sigma-Aldrich. Then the detection was developed by using a secondary antibody conjugated with alkaline phosphatase. Protein bands were visualized using NBT (nitroblue tetrazolium) and BCIP (5-bromo-4-chloro-3-indoyl-phosphate) and their intensity was quantified by densitometric analysis using SMX Image software (BioRad, Hercules, CA). The correct protein loading was ascertained by red Ponceau staining and immunoblotting for β-actin. Cytochrome c oxidase (COX IV) was used as mitochondrial control. All the blots shown are representative of at least three separate experiments.

Analysis of mitochondrial membrane potential

The mitochondrial membrane potential in MDA-MB231 cells was measured using the cationic dye JC-1, which in depolarized mitochondria shows a fluorescence shift from red (emission of JC-1 aggregated form at 590 nm) to green (emission of JC-1 monomeric form at 525 nm). Consequently, the dissipation of mitochondrial membrane potential is indicated by a decrease in the red-to-green fluorescence-intensity ratio. After treatment with compounds, cells (8×10^3/well) were incubated with medium containing JC-1 (Cayman Chemical Company, Ann Arbor, MI) for 15 min at 37°C and then washed twice with PBS. They were then analysed on a Leica DMR fluorescence microscope (Wetzlar, Germany) by using appropriate filters for rhodamine (excitation wavelength of 596 nm and an emission wavelength of 620 nm) and FITC (excitation wavelength of 485 nm and emission wavelength of 530 nm).

Cellular localization of Nrf2 in MDA-MB231 cells by fluorescence microscopy analysis

To assess the intracellular localization of Nrf2 factor, cells (8×10^3/well) were subjected to indirect immunofluorescence analysis in a 96-well plate. Nuclei were visualized by staining the cells with Hoechst 33342 dye (2.5 μg/ml) for 30 min, before the treatment with the compounds. After the treatment the cells were fixed for 5 min with 3% paraformaldehyde and permeabilized with 0.1% Triton X-100 for 5 min at room temperature. The nonspecific binding sites were blocked for 1 h in PBS containing 1% (vol/vol) BSA, after which the fixed cells were incubated overnight at 4 °C with a rabbit polyclonal primary antibody directed against human Nrf2 (Santa Cruz, Ca) diluted 1:100 in PBS. Cells were then washed thrice with PBS and incubated for 2 h with a FITC-conjugated secondary antibody (Santa Cruz, Ca) diluted 1:100 in PBS. Finally, analyses were performed by a Leica DMR fluorescence microscope equipped with a DC300F camera (Leica Microsystems, Wetzlar, Germany). The Hoechst 33342 staining was acquired using DAPI filter (excitation wavelength of 372 nm and emission wavelength of 456 nm), while the Nrf2 staining was visualized by FITC filter (excitation wavelength of 485 nm and emission wavelength of 530 nm). Using Leica Q Fluoro Software (Leica Microsystems), images of the DAPI and FITC fluorescence patterns were merged to visualize intracellular localization of Nrf2 protein.

Statistical analysis

Data are expressed as mean ± S.E. Data were analyzed using the Student's *t*-test. A *P*-value below 0.01 was considered significant.

Results

Pre-treatment with SAHA increased the cytotoxic effect of PN

Our previous studies (D'Anneo et al., 2013b) demonstrated that PN induced in MDA-MB231 cells a cytotoxic effect because it strongly stimulated reactive oxygen species generation. However, the study of the dependence of this effect on PN concentration revealed that at low doses, lower than 10 μM, the cells were scarcely susceptible to the cytotoxic effect. In fact as shown in Figure 1A, 5 μM PN was unable to reduce cell viability in a significant manner also after 72 h of treatment. Therefore we performed some experiments in order to evaluate compounds capable of increasing the cytotoxic effect induced by PN. We demonstrated that the histone deacetylase inhibitor SAHA was very effective in this regard. In particular, we showed that when SAHA and PN were added contemporaneously an additive effect on viability of MDA-MB231 cells was found. Instead, pre-treatment for 20 h with SAHA followed by combined treatment with PN produced a strong synergistic effect. As shown in Figure 1B, pre-treatment of cells with 2 μM SAHA for 20 h decreased cell viability to 85% of control. Addition of 10 μM PN after pre-treatment reduced cell viability; this effect increased with the time of the combined treatment so that after 60 h the cell number decreased to only 3–4% of control. In order to establish whether the treatment with the two compounds produced a synergistic interaction, cells were treated with various doses of SAHA and PN in a fixed ratio (1:5). The effects were compared with those determined by the single compounds. The results reported in Figure 1C were employed to calculate the combination indices (CI) at various values of fraction affected (Fa) (Chou and Talalay, 1984). Figure 1D shows that a synergistic interaction there is between SAHA and PN, because the CI values calculated for the various values of Fa were always inferior to 1. As shown in Figure 1E the addition of the broad spectrum caspase inhibitor z-VAD-fmk at the start of the pre-treatment prevented a great part of the inhibitory effect exerted by the combined treatment on cell viability. Instead necrostatin-1, an inhibitor of RIP-1, exerted only a modest effect. Therefore, our results strongly suggested that the effect on cell viability caused by the combined treatment can be primarily considered as a consequence of the activation of apoptosis. Finally the addition of bafilomycin A1 (BafA1), a powerful inhibitor of the autophagic flux, markedly increased the effect of SAHA on cell viability. In fact, SAHA reduced by 25% the viability of cells when it was added alone and by 70% in the presence of BafA1. This effect of BafA1 led us to the hypothesis that SAHA exerted a role in the survival of the cells by stimulating autophagy.

ROS generation in cells treated with SAHA and PN

The fluorochrome H_2-DCFDA, a general indicator of the level of the reactive oxygen species (ROS), was chosen to ascertain

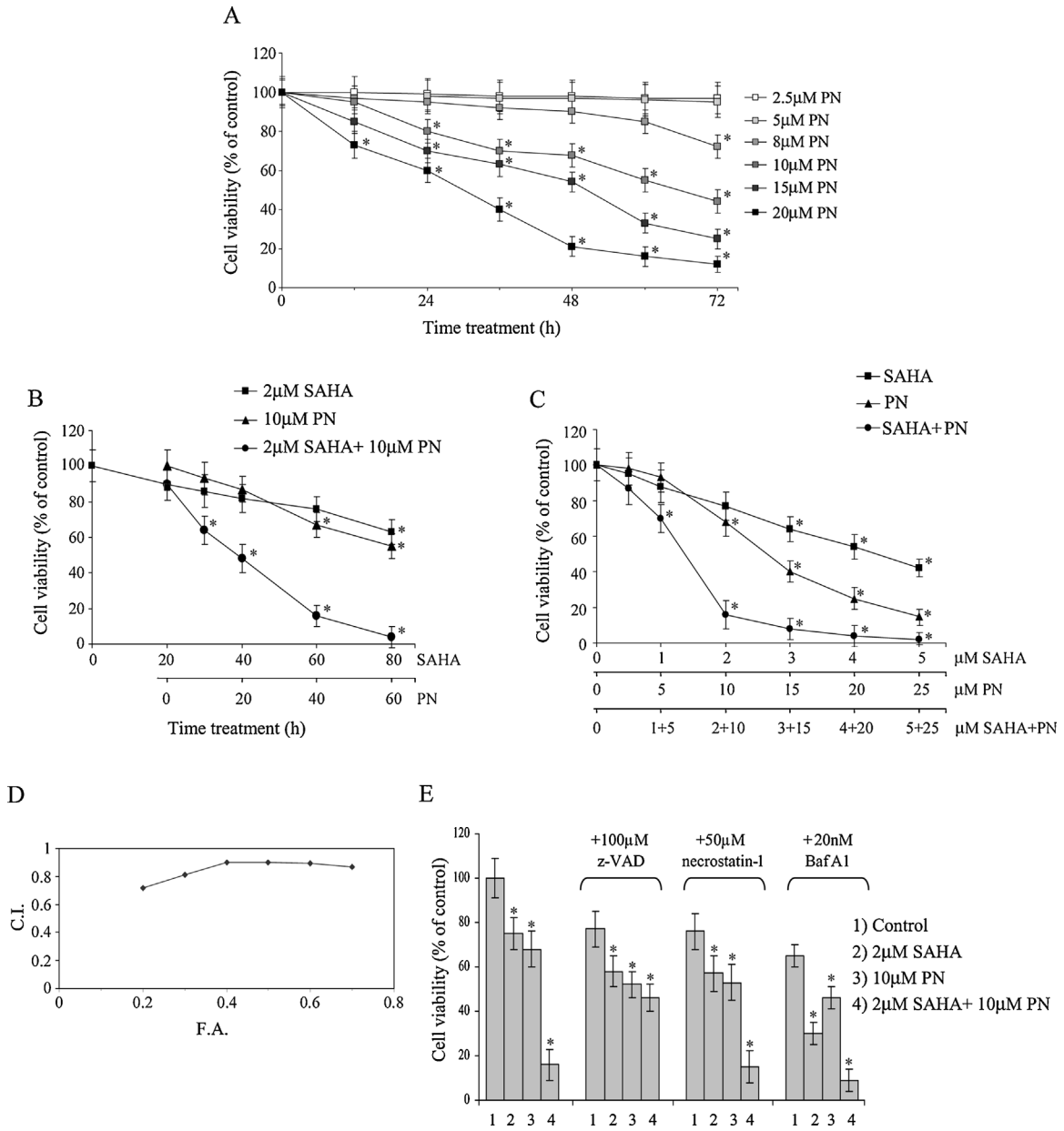

Fig. 1. Treatment with combinations between SAHA and PN induced a strong cytotoxic effect in MDA-MB231 cells. (A) Dose and time dependence of PN effect on cell viability. MDA-MB231 cells (8×10^3/well) were treated for various times with various doses of PN. At the end cell viability was assessed by MTT assay, as reported in Materials and Methods. (B) Pre-treatment with SAHA increased PN effect on cell viability. MDA-MB231 cells were pre-treated for 20 h with 2 μM SAHA. Then 10 μM PN was added and the incubation was protracted for other 20, 40, or 60 h. At the end cell viability was assessed by MTT assay. (C) Comparison of the inhibitory effect on cell viability exerted by various doses of both SAHA and PN alone with that exerted by combinations of the two compounds. Cells were treated with various doses of SAHA (0.5–5 μM) for 60 h or various doses of PN (2.5–25 μM) for 40 h after 20 h with vehicle only. For combined treatments the two compounds were employed in a fixed ratio (1:5, SAHA:PN). After pre-treatment with SAHA for 20 h, cells were treated for other 40 h with SAHA plus PN. At the end viability was assessed by MTT assay. (D) Synergistic effect between SAHA and PN on cell viability. Results shown in Figure 1C were employed to calculate for the different percentages of the inhibitory effect (Fa, fraction affected) the corresponding values of the combination index (CI), in accordance with Chou and Talalay (1984). Since these values were always inferior to 1 we conclude that a synergistic interaction there is between SAHA and PN with regard to the inhibitory effect on cell viability. (E) The influence of z-VAD, necrostatin-1 and BafA1 on the effect exerted by combined treatment with SAHA and PN on the viability of MDA-MB231 cells. Cells were treated for 60 h with the vehicle (1); for 60 h with 2 μM SAHA (2); for 20 h with the vehicle and then for 40 h with 10 μM PN (3); for 20 h with 2 μM SAHA and then for other 40 h with SAHA and PN (4). The effectors (100 μM z-VAD, 50 μM necrostatin-1 and 20 nM BafA1) were added at the start of treatment. At the end viability was assessed by MTT assay. All the values are the means of three independent experiments ± S.E. *$P < 0.01$ compared with control.

ROS generation by direct estimation using fluorescence microscope. We have observed (Fig. 2A and B) that after treatment with 2 μM SAHA about 80% of cells exhibited green fluorescence. Instead, treatment with 10 μM PN alone caused only a very modest production of ROS. Finally combined treatment (SAHA/PN) produced ROS but the effect was lower than that observed with SAHA only. Similar effects were found for all conditions tested after 10–30h of treatment. ROS generation was also observed in the cells prolonging the time of the treatment until 60 h (not shown). The effect was primarily determined by treatment with SAHA alone. Finally the addition of apocynin and DPI, two inhibitors of NADPH oxidase (NOX), partially prevented the effect on ROS generation exerted by SAHA, either when it was employed alone or in combination with PN, whatever the time of incubation was. Because ROS generation was decreased, but not suppressed by apocynin and DPI, we advanced the hypothesis that SAHA could stimulate ROS generation not only through NOX activity, but also at mitochondrial metabolic level, as shown in leukaemia cells by Li et al. 2010.

Autophagy process in cells treated with SAHA and PN

Autophagy can be considered as the major pro-survival mechanism, which is activated in response to many stresses, such as starvation, hypoxia, pathogen infection and chemotherapeutic intervention (Rubinstein and Kimchi, 2012). Our results clearly demonstrate that SAHA strongly induced autophagic process in MDA-MB231 cells. Staining with monodansylcadaverine (MDC) permitted to visualize under fluorescence microscopy the presence of autophagic vacuoles as distinct dot-like structures in the cytoplasm of treated cells. After the treatment with 2 μM SAHA, autophagic vacuoles were clearly observed already at 10 h. Then the number of dot-like structures progressively increased with time until 30 h of treatment, as shown in Figure 3A. Instead, treatment with

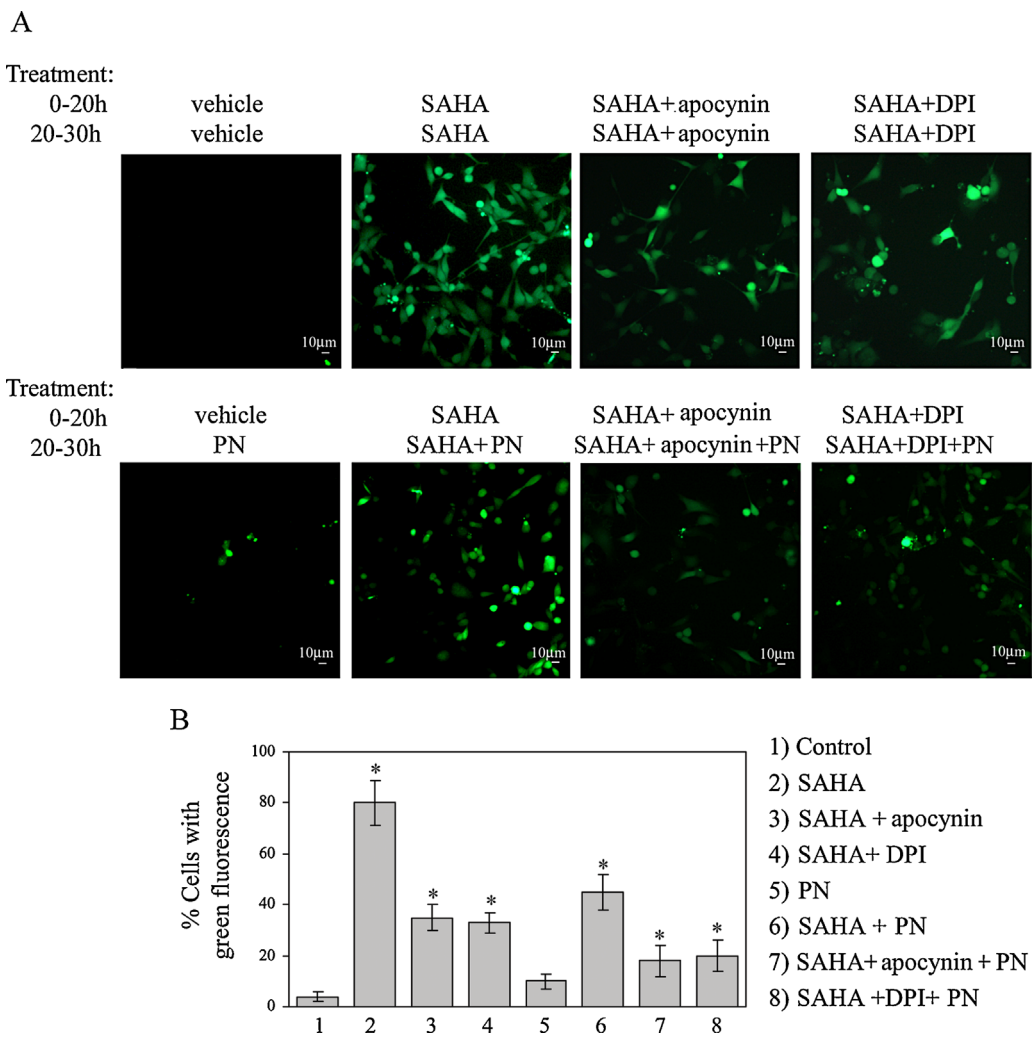

Fig. 2. SAHA stimulated ROS generation in MDA-MB231 cells. Cells (8×10^3/well) were treated for the established times with 2 μM SAHA or 10 μM PN alone or submitted to SAHA/PN combination after a pre-treatment with SAHA alone. The effects of apocynin (100 μM) and DPI (10 μM), two inhibitors of NOX, were also ascertained. At the end, the medium was removed, 100 μl of 50 μM H_2-DCFDA were added and the samples were incubated for other 30 min at 37°C. Then the fluorochrome was substituted with 100 μl PBS and the analysis was performed after 20 min. Oxidation of the fluorochrome produced green fluorescence, which was visualized with a Leica microscope equipped with a DC 300 F camera at × 200 magnification using FITC filter. (A) Images of fluorescence microscopy. Scale bar 10 μm. The results are representative of three independent experiments. (B) Relative percentages of cells with green fluorescence. The values are the means of three independent experiments ± S.E. *$P < 0.01$ compared with vehicle treated control.

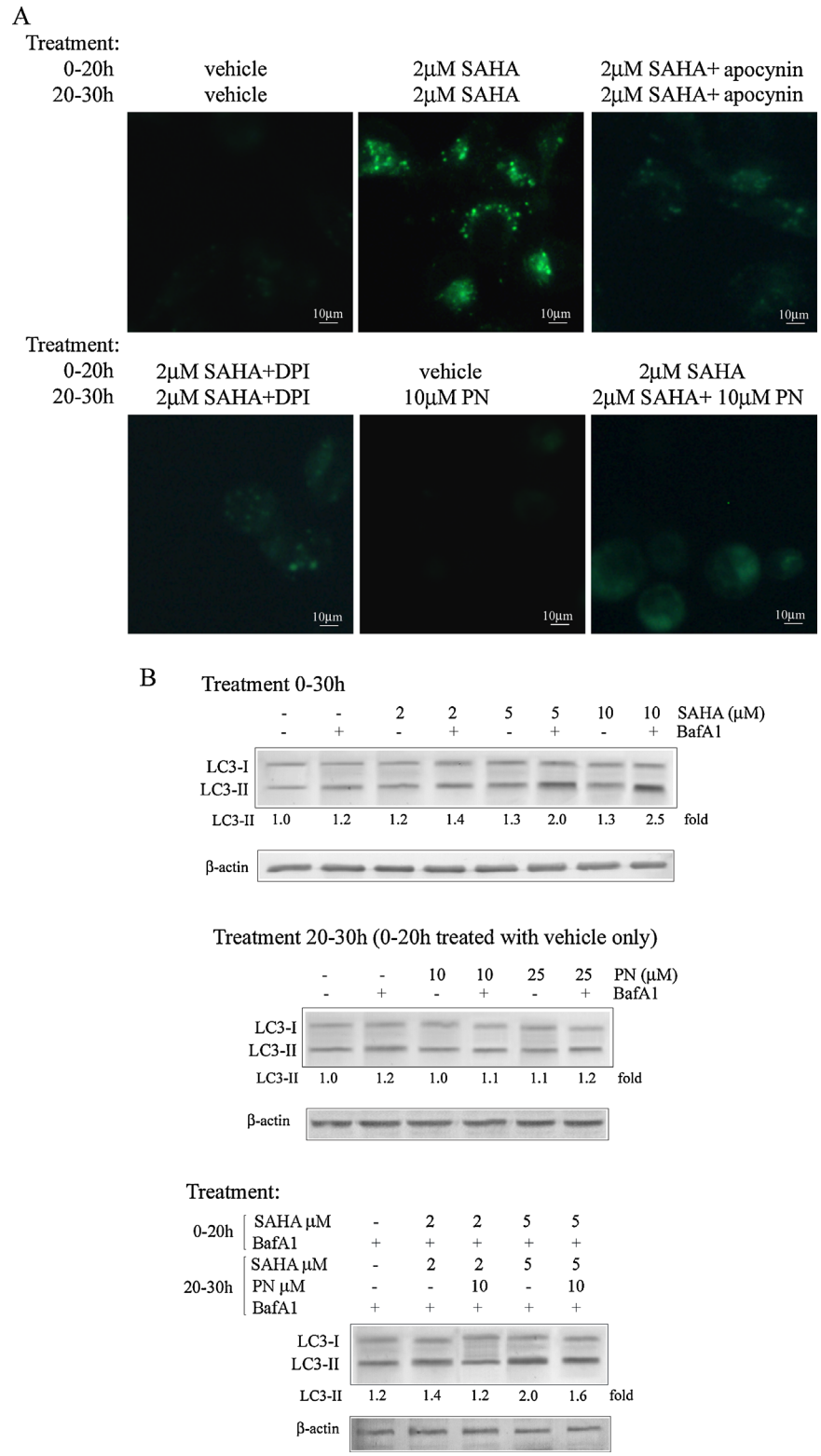

Fig. 3. SAHA stimulated autophagic process in MDA-MB231 cells. Cells (8×10^3/well) were treated with various doses of SAHA or PN alone or submitted to SAHA/PN combination after a pre-treatment with SAHA alone. (A) Detection of autophagic vacuoles with MDC test. The effects of apocynin (100 μM) and DPI (10 μM) were also ascertained. At the end of treatment, the cells were incubated with 50 μM MDC for 10 min. Cell morphology was visualised with a Leica microscope with fluorescence filter for DAPI at × 400 magnification. Scale bar 10 μm. MDC labelled autophagic vacuoles appear as distinct dot-like structures distributed in the cytoplasm. (B) Western blotting analysis showing that treatment with SAHA or SAHA plus PN favoured conversion of LC3-I to LC3-II. The effects were increased by the addition of 20 nM BafA1. Both in (A) and in (B) the results are representative of three independent experiments.

10 μM PN for 10–30 h was unable to stimulate the autophagic process. Finally, SAHA/PN combination reduced the effect observed with SAHA only.

During autophagy, the soluble form of the microtubule-associated protein light chain 3 (LC3-I) is conjugated with phosphatidylethanolammine producing LC3-II. This form is stably associated with autophagosome structure. As shown in Figure 3B, Western blotting analysis demonstrated that 2 μM SAHA favoured accumulation of LC3-II. The effect increased with time from 10 to 30 h of treatment. In addition, our results showed that SAHA caused a flux of autophagy, as suggested by the observation that BafA1 further increased the effect induced by SAHA on LC3-II level.

SAHA alone and in combination with PN induced apoptosis in MDA-MB231 cells

As reported above, autophagic process is activated in response to stress signals. However, if the stress signal is very intense and persistent, autophagic process cannnot ensure survival of the cells. In this condition the mechanism of apoptosis can be triggered leading to elimination of the cells (Rubinstein and Kimchi, 2012). The cysteine proteases, named as caspases (Riedl and Shi, 2004), exert a crucial role in the activation of this process. In order to ascertain whether MDA-MB231 cells underwent apoptosis or necrosis when they were treated with SAHA or PN alone or with SAHA/PN combination, we stained the cells after the treatment with Annexin V- fluorescein isothiocyanate (FITC) and propidium iodide (PI) and analysed by flow cytometry. Figure 4A shows that after treatment with 2 μM SAHA alone for 30 h the cells undergoing early apoptosis (Annexin V-positive/PI- negative cells, C4) amounted to 23.4% of the total while late apoptotic cells (C2) were equal to 11.4% and necrotic cells (C1) only to 1.5%. Treatment with SAHA and PN increased early apoptotic cells to 33.8% and late apoptotic cells to 27.3%, while necrotic cells remained equal to only 1.9%. Finally, these effects were prevented by the addition of z-VAD. The results suggested that treatment with SAHA induced apoptosis and that SAHA/PN combination markedly increased this process. Other experiments were performed in order to ascertain whether combined treatment induced release of cytochrome c and degradation of pro-caspase 3 with the production of the active form of caspase 3 (m.w. 17 kDa) and other cleaved forms. The results shown in Figure 4B demonstrate that treatment with SAHA alone was unable to induce the release of cytochrome c and the activation of caspase 3. Instead, when the cells were treated for 20 h with 2 μM SAHA and then for other 10 h with SAHA/PN combination (lane 4) cytochrome c was released from mitochondria to cytosol. Furthermore, the intensity of pro-caspase 3 band markedly decreased while new bands corresponding to the active form (m.w. 17 kDa) and to a cleaved form (12 kDa) appeared. Both the release of cytochrome c and the activation of caspase 3 were prevented by the addition of z-VAD (lane 5). When the time of the treatment with combinations of SAHA and PN was prolonged to 30 h the band corresponding to pro-caspase 3 disappeared while the intensity of the cleaved forms diminished (not shown). Therefore, these results strongly suggested that treatment with SAHA is capable of inducing primarily early apoptotic effects, relating to the externalization of phosphatidylserine, while combined treatment induces both early and late apoptosis with the release of cytochrome c, cleavage of pro-caspase 3, and production of the active form of caspase 3.

Mitochondrial depolarization and glutathione depletion induced by treatment with PN and SAHA

In order to ascertain a possible role of mitochondria in the mechanism of PN and SAHA treatment, we investigated whether exposure to the drugs was capable of modifying mitochondrial membrane potential ($\Delta\psi m$). For this analysis we used fluorescent cationic dye JC-1 and visualized fluorescence by a Leica microscope. When the cells were treated with 2 μM SAHA (20 h) or 10 μM PN (10 h) alone, red orange fluorescence prevailed on greenish fluorescence, suggesting that most of cells were polarized. Instead, when the cells were pre-treated for 20 h with SAHA and then submitted for other 10 h to combined treatment the greenish fluorescence was predominant. This was evidence that most of the cells were depolarized as a consequence of combined treatment (Fig. 5A). Because it has been suggested that GSH depletion can be responsible for dissipation of $\Delta\psi m$ (Zhang et al., 2004), we analysed whether treatment with the drugs can induce a decrease in the intracellular GSH level. As shown in Figure 5B, when the cells were treated with 2 μM SAHA (30 h) or 10 μM PN (10 h) alone only modest decrements in the intracellular levels of GSH were observed. Instead, when the cells were at first pre-treated for 20 h with SAHA and then submitted for other 10 h to SAHA/PN combination, the level of GSH decreased by 56%.

Crosstalk between autophagy and apoptosis

Autophagy and apoptosis represent two distinct pathways, which are highly interconnected through a constant crosstalk process (Liang et al., 2012; Rubinstein and Kimchi, 2012). Many findings today provided evidence that the cytoprotective function of autophagy is inhibited in many cases by apoptosis, while inhibition of autophagy can lead to the activation of apoptosis (Liang et al., 2012). It is interesting to note that our results suggest that SAHA, in MDA-MB231 cells, induced both autophagy and apoptosis. This observation agrees with many reports showing that SAHA stimulates various tumour cells in both of these processes (Gammoh et al., 2012). In order to study the relationships between autophagy and apoptosis, we examined the effects of the autophagic inhibitor BafA1 on SAHA and PN alone and on SAHA/PN combination. Our results show that the addition of BafA1 to SAHA strongly reduced viability of cells (Fig. 1E). Therefore, the autophagic process induced by SAHA can be considered as a survival mechanism. Moreover, we demonstrated by means of Annexin V/PI test that BafA1 increased the amount of the cells found in both C2 and C4 after treatment with SAHA (Fig. 4A), suggesting that the inhibition of autophagy leads to the increase of the apoptotic death. Therefore, we suggest that a cross-talk occurs in these cells between autophagy and apoptosis.

In addition, it has been shown that some proteins which stimulated autophagic process, such as beclin-1, are cleaved by caspases (Gordy and He, 2012). Cleavage of beclin-1 leads to the inhibition of the cytoprotective autophagy in cells that became committed to apoptosis. In our experiments (Fig. 4C) we demonstrated that the level of beclin-1 was not modified by treatment with SAHA or PN alone, while it decreased after treatment with SAHA/PN combination. Because this effect was prevented by z-VAD we suggest that the apoptotic process activated by SAHA/PN combination can lead, via caspase activation and cleavage of beclin-1, to inhibition of autophagy. In conclusion, with our experimental conditions autophagy seems to be interconnected with apoptosis through mechanisms which regulate both the processes.

Pre-treatment with SAHA suppressed the stimulatory effect of PN on mTOR

AKT/mTOR pathway represents an important survival mechanism that is constitutively activated in many types of cancers (Lo Piccolo et al., 2008). Activation of the serine/treonine kinase AKT is required for different phosphorylation events. The other serine/treonine kinase mTOR (mammalian

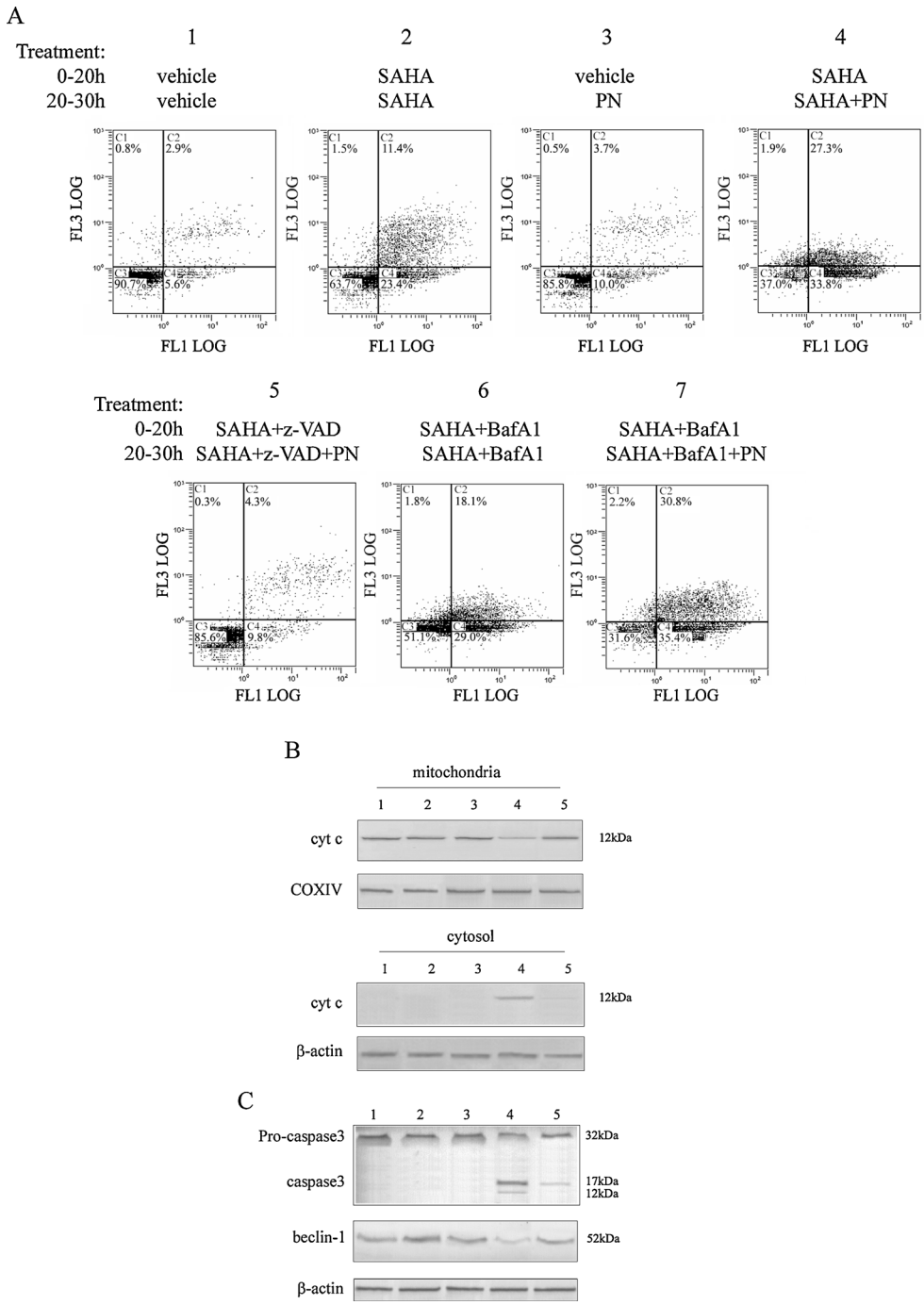

Fig. 4. SAHA alone or in combination with PN stimulated apoptosis in MDA-MB231 cells. Cells were treated for the established times with SAHA or PN alone or submitted to a combined treatment SAHA/PN after a pre-treatment with SAHA alone. (A) Analysis by Annexin V/PI double-staining assay. After treatment, cells were stained with Annexin V-FITC and PI and analysed by flow cytometry. C1 is related to necrotic cells, C2 represents cells in the end stage of apoptosis or necrotic dead cells, C3 were viable cells and finally C4 represents cells undergoing early apoptosis. Treatment with SAHA alone increased the number of cells either in early (C4) and late (C2) apoptosis. Combined treatment with SAHA and PN further increased these effects. The effects were prevented by the addition of 100 μM z-VAD, while they increased in the presence of 20 nM BafA1. (B and C) Western blotting analysis showing the effects induced by SAHA or PN alone or in combination on the levels of cytochrome c (B), pro-caspase 3, caspase 3, and beclin-1 (C). (B) The level of cytochrome c was evaluated both in mitochondrial and cytosolic fractions, which were prepared as reported in Methods. Treatment with SAHA or PN alone did not produce any effect, after treatment with SAHA/PN combination cytochrome c was detected also in the cytosolic fraction, while its level in mitochondrial fraction diminished. (C) For these analyses changes were observed only after combined treatment. In particular caspase 3 and its cleaved form were clearly detected, while the level of pro-caspase 3 decreased. Moreover also the level of beclin-1 markedly diminished. The addition of z-VAD suppressed the changes observed both in (B) and in (C). All the results are representative of three independent experiments.

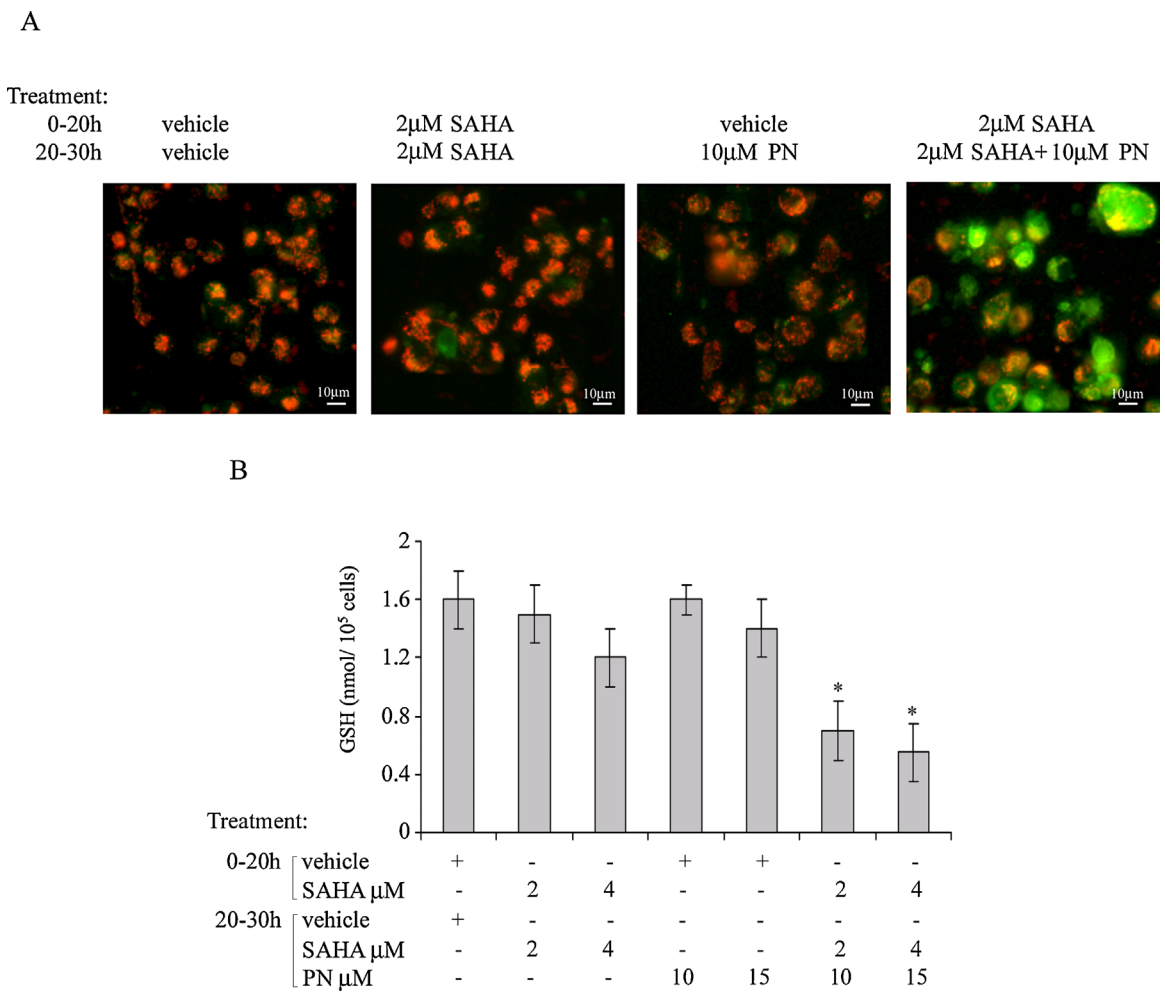

Fig. 5. Combined treatment SAHA/PN induced depolarisation in MDA-MB231 cells and caused depletion of intracellular GSH. Cells were treated for the established times with various doses of SAHA or PN or submitted to a combined treatment after a pre-treatment with SAHA alone. (A) Estimation of mitochondrial membrane potential ($\Delta\psi m$). Determinations were performed using 8×10^3 cells/well. After treatment the fluorochrome JC-1 was added for additional 15 min. Depolarisation was indicated by the shift of fluorescence from red-orange to greenish. Merged images were visualized with a Leica microscope at 200 × magnification with fluorescent filter for FITC and Rhodamine. Scale bar 10 μm. (B) Estimation of the intracellular GSH. 5×10^5 cells were employed for a single sample. At the end of the treatment GSH level was determined by using a colorimetric assay, as reported in Materials and Methods. In (A) the results are representative of three independent experiments. In (B) the values are the means of three independent experiments ± S.E. *$P < 0.01$ compared with vehicle treated control.

target of rapamycin) is the best-studied downstream substrate of AKT. In mammalian cells mTOR is a catalytic component of two distinct complexes mTORC1 and mTORC2. mTORC1 is primarily involved in the control of translation initiation and nutrient sensing (Loewith et al., 2002). This complex is rapamycin sensitive and induces phosphorylation of p70S6K and 4EBP. In addition, mTORC1 inhibits autophagic process by inducing phosphorylation of ULK1/2. In our experiments treatment of MDA-MB231 with 10 μM PN for 10 h resulted in the phosphorylation and activation of AKT, as shown in Figure 6A. In addition, PN induced activation of mTOR pathway, as suggested by the remarkable increase in the level of phospho-mTOR. This effect was accompanied by phosphorylation of p70S6K and S6 ribosomal protein (30 kDa). Finally, PN treatment also induced phosphorylation of ULK1/2. Analysis was performed by using antibodies against phosphorylated forms of AKT, mTOR, p70S6K and S6 protein. It is noteworthy that the levels of the total proteins were not modified by PN treatment (not shown). The presence of the phosphorylated form of ULK1/2 was indicated by the detection of a new band with slower mobility in SDS/PAGE. Our results suggest that exposure to PN activates mTORC1 complex. This conclusion is in accordance with the observations reported by other authors for leukaemia cells (Hassane et al., 2010; Sen et al., 2013). Treatment with SAHA alone caused modest decrements in the levels of phosphorylated forms of AKT, mTOR, p70S6K, S6, and ULK1/2 (Fig. 6A), but pre-treatment with SAHA clearly inhibited the effects exerted by PN on these forms. Therefore, SAHA prevented the activation of AKT/mTOR pathway induced by PN.

Pre-treatment with SAHA suppressed the stimulatory effect of PN on Nrf-2

Next, we investigated whether the cytoprotective effect observed in the presence of low doses of PN can be mediated by Nrf2 (Nuclear factor erythroid 2-related factor 2), a transcription factor (Hassane et al., 2010), which is involved in

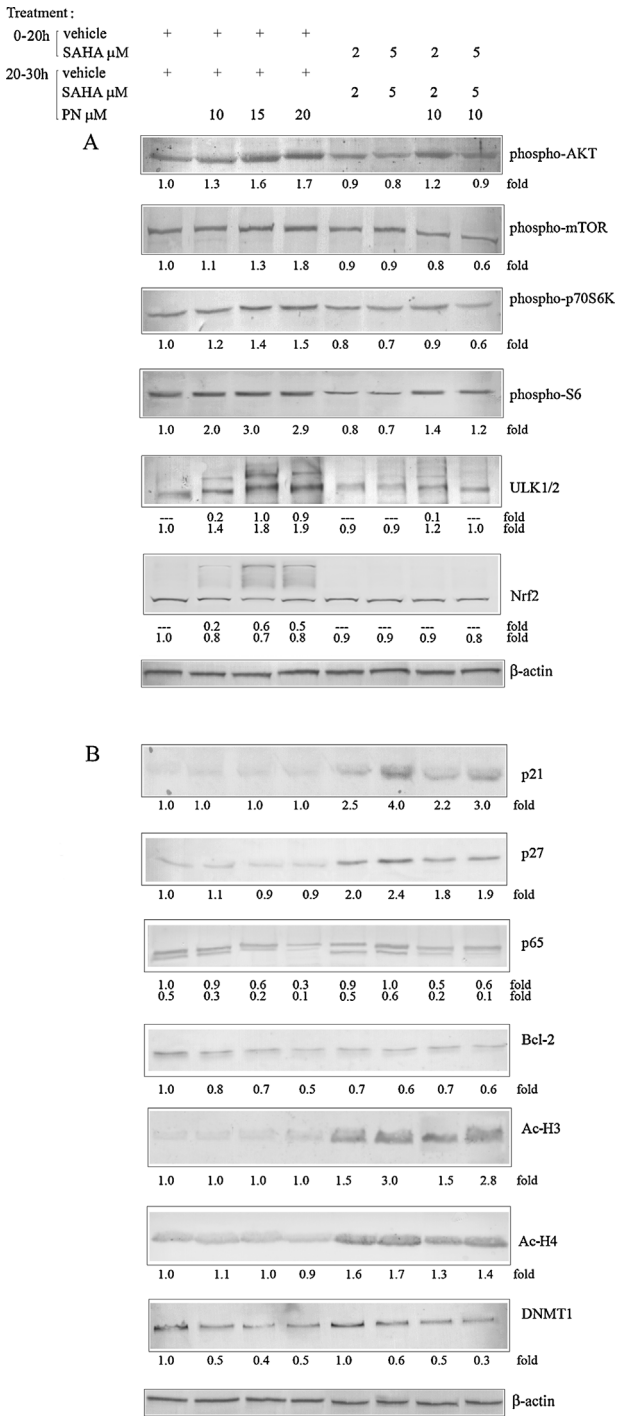

Fig. 6. Western blotting analyses showing changes induced by the treatments on the expression of various factors involved in the molecular mechanisms of the drugs. Cells (1.5×10^5/well) were treated for the established times with various doses of SAHA or PN or submitted to a combined treatment after a pre-treatment with SAHA alone. At the end the extracts were prepared and employed for Western blotting analyses. (A) PN stimulated the mTOR signalling pathway. Pre-treatment with SAHA suppressed this effect. Analysis is related to phospho-AKT (S475), phospho-mTOR (S2448), phospho-p70S6K (T389), phospho-S6, ULK1/2 and Nrf2. (B) Analysis is related to p21, p27, p65, Bcl-2, Ac-H3, Ac-H4, and DNMT1. Both in (A) and (B) the results are representative of three independent experiments.

the basal and induced expression of antioxidant enzyme genes. In unstressed condition, Nrf2 is retained by Keap1 (Kelch-like ECH-associated protein1) in the cytoplasm and committed to proteosomal degradation (Kansanen et al., 2013). In contrast, phosphorylation of Nrf2 by several cytosolic kinases (Pi et al., 2007) stabilizes the protein, which then can translocate into the nucleus where binds to antioxidant-response elements (AREs) in genes encoding for antioxidative enzymes (Nguyen et al., 2003). In accordance with other authors (Hassane et al., 2013; Sen et al., 2013), we advanced the hypothesis that activation of mTOR induced by PN can be responsible for phosphorylation and translocation of Nrf2. In this regard Figure 6A shows that treatment with PN determined the appearance of a new band with slower mobility in SDS/PAGE, which can be identified as a phosphorylated form of Nrf2. This band disappeared when the cells were submitted to SAHA/PN combination. In addition we performed an immunofluorescence approach, staining with an anti-Nrf2 antibody suitable for detection of endogenous Nrf2 (green fluorescence) and with Hoechst 33342 for DNA (bleu fluorescence). As shown in Figure 7A, in MDA-MB231 cells treated with SAHA alone Nrf2 was clearly localized in the cytoplasm, while treatment with PN led to a marked increase of the Nrf2 immunofluorescence signal in the nuclear areas indicating a strong translocation of Nrf2 from the cytoplasm into the nucleus of cells. By contrast, when the cells were pre-treated with SAHA and then exposed to PN, accumulation of Nrf2 in the nucleus was reduced while the immunofluorescence signal was primarily observed in the cytoplasm, thus indicating that the cytoprotective action of PN was counteracted by SAHA.

The effects of the drugs on the expression of various factors involved in the death or in the survival of the cells

Results shown in this paper demonstrate that SAHA and PN in combination synergistically decrease the viability of MDA-MB231 cells. This consideration suggested to us that the two drugs can stimulate the expression of factors involved in the death of tumour cells or inhibit the expression of other proteins involved in cell survival. These events could be a consequence of epigenetic modifications. It is well known that epigenetic changes induced by histone modifications can be responsible for the silencing of tumour suppressor genes while HDAC inhibitors can reactivate these genes and serve as potential anti-cancer drugs (Marks and Xu, 2009; Slingerland et al., 2014). Epigenetic modifications can be also a consequence of changes in DNA methylation. In particular, DNA methylation concerns cytosine residues in the CpG dinucleotide sequences (Robertson, 2005). Abnormal hypermethylation of promoter of tumour suppressor genes has been found in many solid tumors and blood cancers. Further it has been shown that DNA methyl-transferases, and in particular DNMT1, are involved in the aberrant DNA methylation observed in cancer cells (Yoo and Jones, 2006). PN is well known to reduce the level of DNA methylation because it down-regulates the expression of DNMT1 and inhibits its catalytic activity (Liu et al., 2009). Our results demonstrate that treatment with SAHA strongly increased the acetylated forms of histones H3 and H4. In addition, SAHA stimulated the expression of both p21 and p27, two products of tumour suppressor genes and attenuated the level of Bcl-2, an antiapoptotic protein (Fig. 6B). Moreover, we show that 10 μM PN, also after brief treatments (10 h), markedly decreased the expression of DNMT1 (Fig. 6B). In addition, treatment with PN caused a remarkable decrement in the level of p65 and its cleaved form as well as in the level of Bcl-2.

As shown in Figure 7B, we ascertained by Elisa assay, in accordance with a previous finding (D'Anneo et al., 2013b), that PN inhibited DNA-binding activity of p65, a subunit of

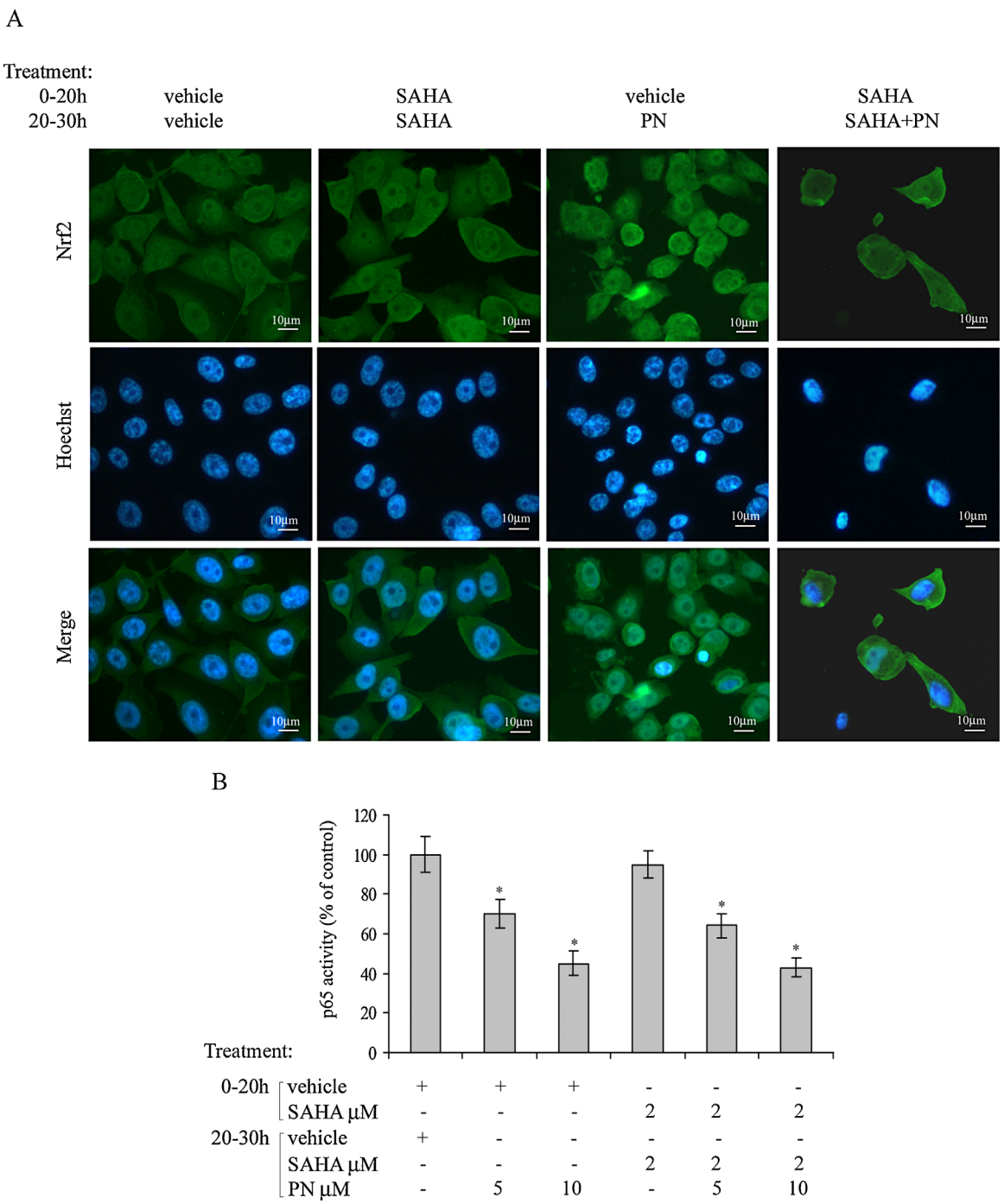

Fig. 7. (A) PN stimulated nuclear translocation of Nrf2. Pre treatment with SAHA suppressed this effect. MDA-MB231 cells (8×10^3 cells) were treated with 2 μM SAHA for 30 h or with 10 μM PN for 10 h. In combined treatment cells were pre-treated with 2 μM SAHA for 20 h, then 10 μM PN was added and the incubation was protracted for another 10 h. After treatment cells were subjected to immunofluorescence analysis of Nrf2 distribution using anti-Nrf2 antibody and FITC conjugated secondary antibody (green fluorescence). Nuclei were stained with Hoechst 33342 (blue fluorescence). The nuclear translocation of Nrf2 was shown by the merge of Nrf2 immunofluorescence and nuclear staining. Fluorescent cells were visualized with a Leica microscope equipped with a DC300F camera at 400× magnification with fluorescent filters for FITC and DAPI for Nrf2 and Hoechst, respectively. Scale bar 10 μm. (B) PN down-regulated DNA-binding activity of p65. Cells (3×10^5/condition) were treated with the drugs, as reported in the legend of Figure 7A. The binding was quantified in nuclear extracts by an Elisa assay as reported in Materials and Methods. The effect of PN was not modified by combination with SAHA. In (A) the results are representative of three independent experiments. In (B) the values are the means of three independent experiments ± S.E. *$P < 0.01$ compared with vehicle treated control.

NF-kB. Treatment with 2 μM SAHA did not modify this activity while treatment with SAHA/PN combination inhibited DNA-binding similarly to PN alone.

In conclusion, treatment with the SAHA/PN combination induced both the hyperacetylation of histones H3 and H4 and the down-regulation of DNMT1 (Fig. 6B). These epigenetic effects were accompanied by the increased expression of the tumour suppressor genes p21 and p27 and by the remarkable decrements in the level of the survival factors Bcl-2 and p65.

Discussion

This study shows that pre-treatment with SAHA strongly increased the cytotoxic effect exerted by PN on viability of MDA-MB231 cells. We provided evidence that a synergistic interaction occurred between SAHA and PN in order to their antitumor action on these cells. The aim of our study was to ascertain the molecular basis of this synergistic effect. Therefore, several aspects of the problem were investigated comparing the effects exerted by PN or SAHA alone to those determined by SAHA/PN combination.

It is well known that both PN and SAHA are capable of inducing epigenetic modifications. PN has been reported (Liu et al., 2009) to inhibit in leukaemia cells DNMT1 through alkylation of cysteine 1226 of the catalytic domain and down-regulation of its expression. These two effects lead to global DNA hypomethylation, which can be effective in modulating the expression of genes involved in the stimulation of apoptotic effects in tumour cells. Our results show that exposure to PN decreased the expression of DNMT1. In addition, PN also decreased the levels of both p65 protein, a component of NF-kB, and Bcl-2 (Wyrębska et al., 2013), a fundamental anti-apoptotic factor.

On the other hand we demonstrated that treatment with SAHA induced acetylation of histones H3 and H4. These results agree with the findings of other authors (Mitsiades et al., 2004; Chen et al., 2013), showing that inhibitors of HDAC increased acetylation of lysine residues in the NH2-terminal tails of histones H3 and H4 with the consequent reactivation of the expression of some silenced genes. Acetylation neutralizes the positive charge of histone tails. Consequently, histone affinity to negative charged DNA diminishes, changes of nucleosome conformation occur and DNA becomes more accessible to transcription factors. In conclusion, histone acetylation can be associated with transcriptionally active regions of the genome. In addition, our results established that histone hyperacetylation induced by SAHA is associated with up-regulation of p21 and p27 as well as with decrement of Bcl-2. These results are also in agreement with previous findings of Bali et al. (2005).

It is noteworthy that treatment with SAHA/PN combination led to the appearance of the modifications induced by both the drugs. Therefore, the cells contemporaneously exhibited both hyperacetylation of histones and decrement of DNMT1 level. These events induce a relatively open structure of chromatin, which can be responsible for epigenetic modifications, favouring changes in the expression of many factors. In particular, we observed that combined treatment was associated with both the increased expression of the tumour suppressor factors p21 and p27 and the decrement in the levels of fundamental survival proteins p65 and Bcl-2. Therefore, we advanced the hypothesis that epigenetic events can be responsible for the changes in the expression of these proteins.

It is well known that NF-kB plays a prominent role in gene expression in tumor cells, favouring survival and metastasis (Baldwin, 2001). Therefore, the antitumor action of PN has been correlated in many tumor cells (Kwok et al., 2001; García-Piñeres et al., 2004) with its inhibitory effect exerted on NF-kB activity. Our results show that PN not only decreased the level of p65, but also inhibited the DNA-binding activity of this protein. It is noteworthy that this remarkable inhibitory effect was not prevent by SAHA when the cells were submitted to SAHA/PN combination.

The experiments concerning the production of ROS and the autophagic process revealed that SAHA alone stimulated both the processes also at low concentrations. Since apocynin and DPI, which are two inhibitors of NOX, reduced both ROS generation and autophagy, we suggest that SAHA primarily stimulated NOX increasing production of ROS, which determined activation of autophagic process. Our results are in agreement with previous reports of other authors, showing that SAHA strongly induces autophagic process in tumour cells (Gammoh et al., 2012).

It is interesting to note that PN at low concentrations (5–8 μM) was unable to stimulate both the production of ROS and the autophagic process, differently from the effect previously observed by us at higher concentration (12–25μM). Moreover, when PN was added to SAHA partially reduced both the effects of this compound on ROS generation and autophagy, while a remarkable activation of apoptosis was observed. In order to explain the mechanism through which PN potentiated apoptosis induced by SAHA, we evaluated the effect of the drugs on mitochondrial membrane potential. When the cells were submitted to combined treatment, a remarkable fall of $\Delta\psi m$ was observed accompanied by a reduction of the intracellular level of GSH. This compound, as shown by Zhang et al. (2004), plays an important role in the stability of mitochondrial membrane potential. Thus, a decrease in the GSH level can be responsible for mitochondrial membrane transition and the consequent fall of $\Delta\psi m$. It is interesting to note that the fall of $\Delta\psi m$ and the decrement of GSH level were observed only when the cells were submitted to combined treatment, but not when they were treated with PN or SAHA alone. However, the mechanism through which combined treatment decreased GSH level is unclear at this moment. Two different modalities can be hypothesized in this regard: oxidation of GSH and conjugation of GSH with PN. Oxidation via ROS generation could be determined at the employed concentrations only by SAHA, while PN was unable to stimulate ROS production and did not increase the effect of SAHA. Conjugation of PN with GSH can occur through its α-methylene-γ-lactone group, but SAHA does not play a role in this regard. Therefore, we believe that both the mechanisms can be involved in the depletion of GSH level. Our results lead us to the conclusion that combined treatment caused fall of $\Delta\psi m$ in correlation with the depletion of GSH. These events together with the activation of the products of the oncosuppressor genes p21 and p27 and the decrements of the levels of the survival proteins p65 and Bcl-2 can be responsible for mitochondrial dysfunction, release of cytochrome c and activation of caspase 3.

Finally, our results show that SAHA/PN combination also induced a decrement of the level of beclin-1, a protein involved in autophagosome formation. It has been shown that beclin-1 is cleaved by caspases (Gordy and He, 2012) and that its N-terminal cleavage fragment can inhibit autophagy while the C-terminal fragment promotes the release of cytochrome c from mitochondria (Wirawan et al., 2010). Thus, it is possible to hypothesize that activation of caspase 3 by SAHA/PN treatment can be responsible for degradation of beclin-1 and that this event can favour the inhibition of the autophagic process activated by SAHA and the release of cytochrome c.

Recently it has been shown that treatment of acute myeloid leukaemia cells with DMAPT induces a cytoprotective response that can decrease the efficacy of this compound. In addition, evidence shows that this cytoprotective effect can be a consequence of activation of the AKT/mTOR pathway in response to PN. This finding suggested that association of PN with compounds capable of inhibiting mTOR pathway can

represent a useful new strategy to impair cytoprotective activity of PN and enhance its antitumor efficacy. Thus, it has been reported that wortmannin (Hassane et al., 2010), an inhibitor of PI3K, as well as some inhibitors of mTOR, such as rapamycin and temsirolimus (Hassane et al., 2010) or the antifungal drug ciclopirox (Sen et al., 2013) enhanced the antileukemic effect of PN by impairing its cytoprotective activity. In a previous paper (D'Anneo et al., 2013b) we have demonstrated that PN induces a decrement of viability of MDA-MB231 cells, which was primarily a consequence of ROS generation. This effect was very modest at a concentration of PN lower than 10 μM. That represented a great limitation for an effective utilization of PN and led us to hypothesize that PN exerts a cytoprotective effect in MDA-MB231 cells by stimulating mTOR pathway and that this protective effect prevails at lower doses of PN, when the drug is unable to stimulate ROS generation. Our results clearly demonstrate that PN is an effective activator of AKT/mTOR pathway inducing its downstream effectors p70S6K and consequently the ribosomal protein S6. Further, when activated by PN, mTOR directly phosphorylates ULK1/2 to inhibit the autophagy function of the ULK complex. The observation that SAHA strongly synergized with PN suggested to us that SAHA can inhibit the activating effect exerted by PN on mTOR. The hypothesis was also supported by the consideration that SAHA is well known to inhibit AKT and mTOR in embryonic fibroblast cells (Gammoh et al., 2012) and in many tumour cells (Hrzenjak et al., 2012; Liu et al., 2010b). Our results, showing that SAHA when employed in combination reduced the effects exerted by PN on mTOR pathway, suggested to us the conclusion that SAHA behaves as an effective inhibitor of mTOR activation.

In addition, our paper shows that PN caused nuclear accumulation of Nrf2, a transcription factor which acts as a key regulator of antioxidant-responsive genes. Treatment with PN stimulated the production of a phosphorylated form of Nrf2, which accumulated in the nucleus. Interestingly, when the cells were submitted to combined treatment, SAHA prevented the effect of PN and the phosphorylated form of Nrf2 was not observed. Therefore, we conclude that PN activated the mTOR pathway and this resulted in the phosphorylation of Nrf2, while SAHA inhibited mTOR activation and consequently Nrf2 phosphorylation.

In conclusion, association between SAHA and PN exhibits several effects concerning viability of MDA-MB231 cells: (i) SAHA and PN together are responsible for epigenetic events which reduced cell viability; (ii) PN inhibits SAHA effect on autophagy; and (iii) SAHA does not modify the inhibitory effect induced by PN on NF-kB, but does suppress the cytoprotective effect of PN by inhibiting AKT/mTOR pathway.

Acknowledgments

This work was supported by grants from: European Regional Development Fund, European Territorial Cooperation 2007-2013, CCI 2007 CB 163 PO 037, OP Italia-Malta 2007-2013; Italian Ministry of Education, University and Research (MIUR) ex-60%, 2012. Dr. D. Carlisi is a recipient of a grant by 'Italian Ministry of Education, University and Research' (MIUR); Dr. G. Buttitta is a PhD student supported by 'Italian Ministry of Education, University and Research' (MIUR); Dr. R. Di Fiore is a recipient of a fellowship granted by the European Regional Development Fund, European Territorial Cooperation 2007–2013, CCI 2007 CB 163 PO 037, OP Italia-Malta 2007–2013.

Literature Cited

Baldwin AS. 2001. Control of oncogenesis and cancer therapy resistance by the transcription factor NF-κB. J Clin Invest 107:241–246.

Bali P, Pranpat M, Swaby R, Fiskus W, Yamaguchi H, Balasis M, Rocha K, Wang HG, Richon V, Bhalla K. 2005. Activity of suberoylanilide hydroxamic acid against human breast cancer cells with amplification of her-2. Clin Cancer Res 11:6382–6389.

Bauer KR, Brown M, Cress RD, Parise CA, Caggiano V. 2007. Descriptive analysis of estrogen receptor (ER)-negative, progesterone receptor (PR)-negative, and HER2-negative invasive breast cancer, the so-called triple-negative phenotype: A population-based study from the California Cancer Registry. Cancer 109:1721–1728.

Bayraktar S, Glück S. 2013. Molecularly targeted therapies for metastatic triple-negative breast cancer. Breast Cancer Res Treat 138:21–35.

Biederbick A, Kern HF, Elsässer HP. 1995. Monodansylcadaverine (MDC) is a specific in vivo marker for autophagic vacuoles. Eur J Cell Biol 66:3–14.

Carlisi D, D'Anneo A, Angileri L, Lauricella M, Emanuele S, Santulli A, Vento R, Tesoriere G. 2011. Parthenolide sensitizes hepatocellular carcinoma cells to TRAIL by inducing the expression of death receptors through inhibition of STAT3 activation. J Cell Physiol 226:1632–1641.

Carlisi D, D'Anneo A, Martinez R, Emanuele S, Buttitta G, Di Fiore R, Vento R, Tesoriere G, Lauricella M. 2014. The oxygen radicals involved in the toxicity induced by parthenolide in MDA-MB-231 cells. Oncol Rep 32:167–172.

Chen S, Zhao Y, Gou WF, Zhao S, Takano Y, Zheng HC. 2013. The anti-tumor effects and molecular mechanisms of suberoylanilide hydroxamic acid (SAHA) on the aggressive phenotypes of ovarian carcinoma cells. PLoS ONE 8:e79781.

Chou TC, Talalay P. 1984. Quantitative analysis of dose-effect relationships: The combined effects of multiple drugs or enzyme inhibitors. Adv Enzyme Regul 22:27–55.

D'Anneo A, Carlisi D, Lauricella M, Emanuele S, Di Fiore R, Vento R, Tesoriere G. 2013a. Parthenolide induces caspase-independent and AIF-mediated cell death in human osteosarcoma and melanoma cells. J Cell Physiol 228:952–967.

D'Anneo A, Carlisi D, Lauricella M, Puleio R, Martinez R, Di Bella S, Di Marco P, Emanuele S, Di Fiore R, Guercio A, Vento R, Tesoriere G. 2013b. Parthenolide generates reactive oxygen species and autophagy in MDA-MB231 cells. A soluble parthenolide analogue inhibits tumour growth and metastasis in a xenograft model of breast cancer. Cell Death Dis 4:e891.

Dey N, Smith BR, Leyland-Jones B. 2012. Targeting basal-like breast cancers. Curr Drug Targets 13:1510–1524.

Emanuele S, Lauricella M, Carlisi D, Vassallo B, D'Anneo A, Di Fazio P, Vento R, Tesoriere G. 2007. SAHA induces apoptosis in hepatoma cells and synergistically interacts with the proteasome inhibitor Bortezomib. Apoptosis 12:1327–1338.

Gammoh N, Lam D, Puente C, Ganley I, Marks PA, Jiang X. 2012. Role of autophagy in histone deacetylase inhibitor-induced apoptotic and nonapoptotic cell death. Proc Natl Acad Sci U S A 109:6561–6565.

García-Piñeres AJ, Lindenmeyer MT, Merfort I. 2004. Role of cysteine residues of p65/NF-kB on the inhibition by the sesquiterpene lactone parthenolide and N-ethyl maleimide, and on its transactivating potential. Life Sciences 75:841–856.

Ghantous A, Sinjab A, Herceg Z, Darwiche N. 2013. Parthenolide: From plant shoots to cancer roots. Drug Discov Today 18:894–905.

Gordy C, He YW. 2012. The crosstalk between autophagy and apoptosis: Where does this lead. Protein Cell 3:17–27.

Guerrant W, Patil V, Canzoneri JC, Oyelere AK. 2012. Dual targeting of histone deacetylase and topoisomerase II with novel bifunctional inhibitors. J Med Chem 55:1465–1477.

Guzman ML, Rossi RM, Neelakantan S, Li X, Corbett CA, Hassane DC. 2007. An orally bioavailable parthenolide analog selectively eradicates acute myelogenous leukemia stem and progenitor cells. Blood 110:4427–4435.

Hassane DC, Sen S, Minhajuddin M, Rossi RM, Corbett CA, Balys M, Wei L, Crooks PA, Guzman ML, Jordan CT. 2010. Chemical genomic screening reveals synergism between parthenolide and inhibitors of the PI-3 kinase and mTOR pathways. Blood 116:5983–5990.

Hrzenjak A, Kremser ML, Strohmeier B, Moinfar F, Zatloukal K, Denk H. 2008. SAHA induces caspase-independent, autophagic cell death of endometrial stromal sarcoma cells by influencing the mTOR pathway. J Pathol 216:495–504.

Kansanen E, Kuosmanen SM, Leinonen H, Levonen AL. 2013. The Keap1-Nrf2 pathway: Mechanisms of activation and dysregulation in cancer. Redox Biol 1:45–49.

Kwok BH, Koh B, Ndubuisi MI, Elofsson M, Crews CM. 2001. The anti-inflammatory natural product parthenolide from the medicinal herb Feverfew directly binds to and inhibits IκB kinase. Chem Biol 8:759–766.

Lauricella M, Ciraolo A, Carlisi D, Vento R, Tesoriere G. 2012. SAHA/TRAIL combination induces detachment and anoikis of MDA-MB231 and MCF-7 breast cancer cells. Biochimie 94:287–299.

Li J, Liu R, Lei Y, Wang K, Lau QC, Xie N, Zhou S, Nie C, Chen L, Wei Y, Huang C. 2010. Proteomic analysis revealed association of aberrant ROS signaling with suberoylanilide hydroxamic acid-induced autophagy in Jurkat T-leukemia cells. Autophagy 6:711–724.

Liang B, Kong D, Liu Y, Liang N, He M, Ma S, Liu X. 2012. Autophagy inhibition plays the synergetic killing roles with radiation in the multi-drug resistant SKVCR ovarian cancer cells. Radiat Oncol 7:213.

Liu JW, Cai MX, Xin Y, Wu QS, Ma J, Yang P, Xie HY, Huang DS. 2010a. Parthenolide induces proliferation inhibition and apoptosis of pancreatic cancer cells in vitro. J Exp Clin Cancer Res 29:108.

Liu Z, Liu S, Xie Z, Pavlovicz RE, Wu J, Chen P, Aimiuwu J, Pang J, Bhasin D, Neviani P, Fuchs JR, Plass C, Li PK, Li C, Huang TH, Wu LC, Rush L, Wang H, Perrotti D, Marcucci G, Chan KK. 2009. Modulation of DNA Methylation by a Sesquiterpene Lactone Parthenolide. J Pharmacol Exp Ther 329:505–514.

Liu YL, Yang PM, Shun CT, Wu MS, Weng JR, Chen CC. 2010b. Autophagy potentiates the anti-cancer effects of the histone deacetylase inhibitors in hepatocellular carcinoma. Autophagy 6:1057–1065.

Lo Piccolo J, Blumenthal GM, Bernstein WB, Dennis PA. 2008. Targeting the PI3K/Akt/mTOR pathway: Effective combinations and clinical considerations. Drug Resist Updat 11:32–50.

Loewith R, Jacinto E, Wullschleger S, Lorberg A, Crespo JL, Bonenfant D, Oppliger W, Jenoe P, Hall MN. 2002. Two TOR complexes, only one of which is rapamycin sensitive, have distinct roles in cell growth control. Mol Cell 10:457–468.

Lowry OH, Rosebrough NJ, Farr AL, Randall RJ. 1951. Protein measurement with the folin phenol reagent. J Biol Chem 193:265–275.

Marks PA, Xu WS. 2009. Histone deacetylase inhibitors: Potential in cancer therapy. J Cell Biochem 107:600–608.

Mitsiades CS, Mitsiades NS, McMullan CJ, Poulaki V, Shringarpure R, Hideshima T, Akiyama M, Chauhan D, Munshi N, Gu X, Bailey C, Joseph M, Libermann TA, Richon VM, Marks PA, Anderson KC. 2004. Transcriptional signature of histone deacetylase inhibition in multiple myeloma: biological and clinical implications. Proc Natl Acad Sci U S A 101:540–545.

Nguyen T, Sherratt PJ, Pickett CB. 2003. Regulatory mechanisms controlling gene expression mediated by the antioxidant response element. Annu Rev Pharmacol Toxicol 43:233–260.

Pi J, Bai Y, Reece JM, Williams J, Liu D, Freeman ML, Fahl WE, Shugar D, Liu J, Qu W, Collins S, Waalkes MP. 2007. Molecular mechanism of human Nrf2 activation and degradation: Role of sequential phosphorylation by protein kinase CK2. Free Radic Biol Med 42:1797–1806.

Riedl SJ, Shi Y. 2004. Molecular mechanisms of caspase regulation during apoptosis. Nat Rev Mol Cell Biol 5:897–907.

Robertson KD. 2005. DNA methylation and human disease. Nat Rev Genet 6:597–610.

Rubinstein AD, Kimchi A. 2012. Life in the balance - a mechanistic view of the crosstalk between autophagy and apoptosis. J Cell Sci 15:5259–5268.

Sen S, Hassane DC, Corbett C, Becker MW, Jordan CT, Guzman ML. 2013. Novel mTOR inhibitory activity of ciclopirox enhances parthenolide antileukemia activity. Exp Hematol 41:799–807.

Shanmugam R, Kusumanchi P, Appaiah H, Cheng L, Crooks P, Neelakantan S, Peat T, Klaunig J, Matthews W, Nakshatri H, Sweeney CJ. 2011. A water soluble parthenolide analog suppresses in vivo tumor growth of two tobacco-associated cancers, lung and bladder cancer, by targeting NF-kB and generating reactive oxygen species. Int J Cancer 128:2481–2494.

Shanmugam R, Kusumanchi P, Cheng L, Crooks P, Neelakantan S, Matthews W, Nakshatri H, Sweeney CJ. 2010. A water-soluble parthenolide analogue suppresses in vivo prostate cancer growth by targeting NFkappaB and generating reactive oxygen species. Prostate 70:1074–1086.

Slingerland M, Guchelaar HJ, Gelderblom H. 2014. Histone deacetylase inhibitors: An overview of the clinical studies in solid tumors. Anticancer Drugs 25:140–149.

Sun Y, St Clair DK, Xu Y, Crooks PA, St Clair WH. 2010. A NADPH oxidase-dependent redox signaling pathway mediates the selective radiosensitization effect of parthenolide in prostate cancer cells. Cancer Res 70:2880–2890.

Suvannasankha A, Crean CD, Shanmugam R, Farag SS, Abonour R, Boswell HS, Nakshatri H. 2008. Antimyeloma effects of a sesquiterpene lactone parthenolide. Clin Cancer Res 14:1814–1822.

Wirawan E, Vande Walle, Kersse L, Cornelis K, Claerhout S, Vanoverberghe S, Roelandt I, De Rycke R, Verspurten R, Declercq J, Agostinis W, Vanden P, Berghe T, Lippens S, Vandenabeele P. 2010. Caspase-mediated cleavage of Beclin-1 inactivates Beclin-1-induced autophagy and enhances apoptosis by promoting the release of proapoptotic factors from mitochondria. Cell Death Dis 1:e18.

Wyrębska A, Szymański J, Gach K, Piekielna J, Koszuk J, Janecki T, Janecka A. 2013. Apoptosis-mediated cytotoxic effects of parthenolide and the new synthetic analog MZ-6 on two breast cancer cell lines. Mol Biol Rep 40:1655–1663.

Yoo CB, Jones PA. 2006. Epigenetic therapy of cancer: past, present and future. Nat Rev Drug Discov 5:37–50.

Zhang S, Ong CN, Shen HM. 2004. Critical roles of intracellular thiols and calcium in parthenolide-induced apoptosis in human colorectal cancer cells. Cancer Lett 208:143–153.

Zunino SJ, Ducore JM, Storms DH. 2007. Parthenolide induces significant apoptosis and production of reactive oxygen species in high-risk pre-B leukaemia cells. Cancer Lett 254:119–127.